Thermal stability of Al2MgC2 and thermodynamic modeling of the Al–C–Mg system - Application to grain refinement of Mg–Al alloys

G. Deffrennes, B. Gardiola, M. Lomello-Tafin, A. Pasturel, A. Pisch, J. Andrieux, R. Schmid-Fetzer, O. Dezellus

Thermal stability of Al_2MgC_2 and thermodynamic modeling of the Al-C-Mg system - Application to grain refinement of Mg-Al alloys

G. Deffrennes[1], B. Gardiola[1], M. Lomello-Tafin[4], A. Pasturel[2], A. Pisch[2], J. Andrieux[1], R Schmid-Fetzer[3], O. Dezellus[1]

[1] Univ. Claude Bernard Lyon 1, CNRS, LMI, 69100 Villeurbanne, France

[2] Univ. Grenoble Alpes, CNRS, Grenoble INP, SIMAP, 38000 Grenoble, France

[3] Institute of Metallurgy, Clausthal University of Technology, Robert-Koch-Str. 42, D-38678 Clausthal-Zellerfeld, Germany

[4] SYMME, Université Savoie Mont Blanc, BP. 80439, 74944 Annecy-Le-Vieux Cedex, France

Abstract

In the scope of supporting the development of Mg-Al alloys and related materials, an experimental study coupled with a CALPHAD thermodynamic modeling of the Al-C-Mg system was conducted. The peritectic decomposition of Al_2MgC_2 to form Al_4C_3, graphite and a liquid phase was measured at 1559±10 K by DTA. In order to model the Mg solubility in Al_4C_3, DFT calculations were performed on the end-member phases Mg_4C_3, $Al_2Mg_2C_3$ and $Mg_2Al_2C_3$ and it was shown that Mg substitutes on the Al2 crystallographic site of the carbide structure. Based on recent literature data and a revised Al-C binary, a model description of the Al-C-Mg ternary is proposed for the first time. More specifically, it is used to calculate the liquidus projection and the phase formation sequence during Scheil solidification of a 91Mg-9Al wt% alloy inoculated with carbon. This work provides a convincing argument that Al_2MgC_2 is the nucleant responsible for the grain refinement of Mg-Al alloys inoculated by C.

1. Introduction

The Al-C-Mg system supports exciting perspectives for electronic and functional materials and is the cornerstone of important industrial applications for structural materials.

First of all, challenging yet appealing pioneer research can be made on the carbides of the ternary system. On the one hand, there is the prospect of an application of Al-C-Mg carbides in electronic. Al_4C_3 and Al_2MgC_2 are semiconductors with an indirect band gap calculated by DFT at respectively 1.34 [1] and 1.73 eV [2], although it is to be noted that those values are very likely to be underestimated. Plus, Al_4C_3 can contain a significant amount of Mg in solid solution [2,3] pointing to the possibility of a p-type doping. Finally, the hexagonal structure of Al_4C_3 and Al_2MgC_2 suggests a good compatibility with the 4H polytype of SiC in the scope of making heterojunctions by epitaxial growth. On the other hand, the crystal structure of Al_2MgC_2 is made of Al-C layers separated by weakly bonded Mg layers [2]. As a result, the delamination of the structure to make 2D materials similarly to the synthesis of MXenes from MAX phases [4,5] can be considered.

Then, Mg-based composite are promising materials in lightweight applications [6]. For such materials, the phase formation at the fibre-matrix interface is determinant to the mechanical properties of the assembly [7]. In the case of Mg-Al matrix composites reinforced by carbon fibres, the formation of Al_2MgC_2 was shown to have a considerable effect on mechanical properties by changing the matrix/fibre bonding strength [8–10] or by consuming alloying elements [11].

Besides, the main industrial interest of the Al-C-Mg ternary lies in the grain refinement potential in Mg-Al alloys by means of carbon inoculation. This has been an active research topic for the last 20 years as this technique was proven to be the most promising alternative to the use of Zr which forms intermetallics with Al. Remarkable

improvements of strength and ductility [12–15], creep resistance [16], corrosion resistance [17] and even hot working processing [18,19] of Mg-Al alloys were obtained by refining their microstructure. However, underlying mechanisms of the refinement has been widely disputed in the literature.

First of all, Jin et al. [20] focused on the role of carbon as a solute. This mechanism was further debated between Qian et al. [21] and Jin et al. [22] and was contested by Kim et al. [23]. Afterwards, it was widely accepted that carbon inoculation refines Mg-Al microstructures by promoting the heterogeneous nucleation of α-Mg. Nonetheless, the nature of the potent nucleant particle was extensively debated. In a first place, Al_2OC was considered by Qian et al. [21], yet its formation was argued to be unlikely from a thermodynamic point of view [22,24,25]. Then, another issue lies in the role of Mn as an alloying element. Some authors [23,26] consider its presence a prerequisite for achieving refinement and a duplex nucleation theory revolving around the Al_8Mn phase was proposed. However, many authors could obtained refined microstructures without additions of Mn [13,21,24,25] and Easton et al. [27] even considered Mn to poison the grain refining effect of carbon. In addition, the duplex nucleation theory was contested by experimental evidence from Wang et al. [28]. Finally, the Al_4C_3 carbide was widely considered to be the nucleant responsible for the refinement [13,15,24–31]. Yet recently, Huang et al. [32] investigated Mg-Al alloys inoculated by SiC and characterized by TEM the presence of Al_2MgC_2 existing in a crystallographic orientation relationship with the α-Mg matrix. It is also noteworthy that epitaxial growth of Mg on Al_2MgC_2 was already reported 10 years before that by Cayron et al. [33] when studying Mg-Al composites. All in all, extensive researches were conducted regarding the grain refinement of Mg-Al alloys by carbon inoculation and the debate is still open.

In spite of the major industrial interest of the Al-C-Mg ternary system, a complete thermodynamic assessment of Al-C-Mg have yet to be proposed as neither Al_2MgC_2 nor the solubility of Mg in Al_4C_3 [2,3] is currently described in commercial databases [34–36]. This shortage surely fueled the debate on the grain refinement of Mg-Al alloys by carbon inoculation as one cannot rely on thermodynamic calculations to support very delicate experimental work. Indeed, Mg high vapor pressure and reactivity have to be dealt with as well as the fact that Al_4C_3 [37,38] and Al_2MgC_2 [3,32] undergo hydrolysis in ambient air.

In the scope of the thermodynamic modeling of the Al-C-Mg system, experimental investigations coupled with DFT calculations on the thermodynamic properties of Al_4C_3 [1] and Al_2MgC_2 [2] were recently performed. Notably, the thermodynamic description of the Al-C system was revised [39] as conflicting results could be found regarding the enthalpy of formation of Al_4C_3 [1] and phase equilibria [39].

After a preliminary result recently published by Deffrennes et al. [40], a reliable invariant decomposition temperature of Al_2MgC_2 is confirmed in the present study by the mean of Differential Thermal Analysis (DTA). In order to model the solubility of Mg in Al_4C_3, the standard enthalpy of formation of potential end-members phases is calculated by DFT. Based on those results and on recent work [2] as well as on the revised description of the Al-C binary [39], the Al-C-Mg system is modeled, and descriptions for Al_2MgC_2 and for the solubility of Mg in Al_4C_3 are proposed for the first time. Finally, thermodynamic calculations are performed to contribute to the grain refinement debate of Mg-Al alloys by carbon inoculation.

2. Assessment of literature data

2.1 Solid phases

The known stable solid phases of the Al-C-Mg system are listed in Table 1. Data are given according to references [3,39,41–53].

Table 1 Stable solid phases of the Al-C-Mg system and their crystal structure under 1 bar

Phase/ Temp. range (K)	Pearson Symbol/ Space Group/ Prototype	Lattice parameters (pm)	Comments
(Al) < 933.45 [50]	*cF*4 $Fm\overline{3}m$ Cu	a=404.961	At T=298 K, [40] Up to 18.6 at.% Mg at 723 K [41]
(Mg) < 923.00 [50]	*hP*2 $P6_3/mmc$ Mg	a=320.93 c=521.03	At T=298 K, [40] Up to 11.8 at.% Al at 710 K [41]
Graphite, C 3895 < T_{sub} < 4020 [51]	*hP4* $P6_3/mmc$ C (graphite)	a=246.4(2) b=671.1(4)	At T=300 K, Neutron diffraction [42]
β, Mg_2Al_3 < 723 [44]	*cF*1168 $Fd\overline{3}m$ β-Mg_2Al_3	a=2823.9±0.001	At T=296±1 K and 60.3 at.% Al, powder XRD [45] 59-62 at.% Al [43]
γ, $Mg_{17}Al_{12}$ < 731 [43]	*cI*58 $I\overline{4}3m$ α-Mn	1050 < a < 1066	Kikuchi diffraction (TEM) [49] 39.5 [41] < at.% Al < 54.2 at.% [43]
ε, $Mg_{23}Al_{30}$ 523 < T < 683 [43]	*hP*159 $R\overline{3}$ $Mn_{44}Si_9$	a=1282.54±0.0003 c=2174.78±0.0009	Powder XRD [46] 54-56 at.%Al [44]
Al_4C_3 < 2425 [39]	*hP*21 $R\overline{3}m$ Al_4C_3	a=333.5(1) c=2496.7(3)	At T=298 K and 0 at.% Mg, single-crystal XRD [47] Up to approx. 4.7 at.% Mg at 1000 K [3], calculated at 4.4 at.% Mg in this work
T1-Al_2MgC_2 T < 1000 [49]	*hP*10 $P6_3/mmc$ β-Be_3N_2	a=340.17(7) c=1229.2(2)	At T=298 K, Powder XRD [49] Space group was proposed by [9] A mixture between T1 and T2 is obtained between 930 and 1000 K [49]
T2-Al_2MgC_2 930 [49] < T < 1559 (this work)	*hP*5 $P\overline{3}m1$ Al_3Ni_2	a=337.67(11) c=580.7(2)	T=150 K, XRD on single-crystal obtained after quenching [2] A mixture between T1 and T2 is obtained between 930 and 1000 K [49] Thermal stability measured under 3.4 bar at 1559±10 K and calculated at 1550 K in this work

2.2 The Al-C binary system

The data regarding the Al-C binary system were recently reviewed by Deffrennes et al. [39] who pointed out significant discrepancies in the literature results on phase equilibria and on the standard enthalpy of formation of Al_4C_3. Then, a thermodynamic description was proposed by the authors [39] on the basis of this critical selection of literature data along with some new measurements and DFT calculations.

2.3 The Al-Mg binary system

The literature regarding the Al-Mg system was critically reviewed by Murray [42] in 1982. Since then, experimental studies focusing on the central part of the diagram were conducted [44,45]. Those results were taken into account in the most recent description of the Al-Mg binary proposed by Aljarrah [54] who used the modified quasi-chemical model to describe the liquid phase. The results of Aljarrah's modeling are rather similar with those from the description given in the COST507 database [55] where a substitutional solution model was used for the liquid phase. The later description is therefore selected in this work as the same model is used to describe the liquid phase.

2.4 The C-Mg binary system

The data regarding the C-Mg binary were critically assessed by Chen et al. [56] and a thermodynamic description of the system was provided by the authors. This evaluation is based on recent measurements of the limited carbon solubility in liquid Mg [57] and includes descriptions for the metastable magnesium carbides.

2.5 The Al-C-Mg ternary system

Due to challenging experimental work, information on the Al-C-Mg system are scarce. Above the melting points of Al and Mg, Al_2MgC_2 and Al_4C_3 are the only stable solid phases besides graphite in the ternary system. Al_2MgC_2 is stoichiometric [2,3,49] and exists under two polymorphic forms so-called T1 and T2 in the literature [49]. The T2 form is obtained exclusively above 1000 K, and a mixture between T1 and T2 is obtained at temperatures below, T1 being the dominant form up to 990 K [49]. In the ternary, Al_4C_3 can contain a significant amount of Mg of up to roughly 6 wt% in solid solution at 1000 K [3]. Firstly, information regarding the thermodynamic properties of the Al_2MgC_2 ternary carbide will be reviewed, while in a second time, the data regarding phase equilibria will be considered.

The structure and thermodynamic properties of T2-Al_2MgC_2 were recently investigated by Deffrennes et al. [2]. The enthalpy of formation of the phase was predicted by DFT to be -23.6 kJ.mol of atoms^{-1} using the recent Strongly Constrained and Appropriately Normed (SCAN) functional [58,59]. Phonon calculation in the quasi-harmonic approximations were performed from 0 to 1000 K leading to the heat capacity of the phase and the standard entropy of formation of T2-Al_2MgC_2 was found to be 70.0 J.mol^{-1}.K^{-1} [2]. Below 300 K, previous results on Al_4C_3 [1] that were found in very good agreement with the experimental literature data support the validity of the calculations performed by the authors on the ternary carbide. From 300 to 871 K, DSC measurements were also performed by Deffrennes et al. [2] and a satisfying agreement was obtained between the DFT and DSC results. However, due to insufficient knowledge of the impurities proportion in the measured sample, an uncertainty of 5% was associated with the DSC measurements. Therefore, the phonon calculations are preferred over the DSC measurements in the present assessment even though the heat capacity might be underestimated at high temperatures due to anharmonic contributions.

The lattice parameters of T1-Al_2MgC_2 were determined by Bosselet et al. [49] and its atomic parameters were proposed by Feldhoff et al. [53]. Unfortunately, very limited information are available regarding the T1-Al_2MgC_2 form, notably as it cannot be synthesized free of T2. As a result, only the T2 variety will be considered in this work in the whole temperature range. Nonetheless, it is very interesting to note that attempts made to observe a reversible transition between T1 and T2 by re-heating samples in the polymorphs respective temperature range of existence failed [3,49]. The authors [3,49] concluded that the two forms exhibit a certain metastable character, similarly to the case of cubic and hexagonal forms of SiC. Therefore, even though only the T2 form is considered in the present modeling, it is likely that the energy difference between T1 and T2 is very small and that the equilibria involving the T1 form would not vary significantly from the ones calculated in this work.

Phase equilibria in the Al-C-Mg system were studied at 1000 K by Viala et al. [3] and an experimental isothermal section was proposed. The authors [3] measured the phase composition of various samples by WDS after natural cooling. First of all, Viala et al. [3] determined a composition of 0.6+/-0.2 wt%Al for the liquid involved in three-phase equilibria with graphite and T2-Al_2MgC_2 at 1000 K. This value is in reasonable

agreement with the value of 2.3 wt% recently measured at 1273 K by EDS by Deffrennes et al. [2]. Regarding the liquid in equilibria with Al_4C_3 and T2-Al_2MgC_2, Viala et al. [3] found an Al content of 19+/-2 wt% at 1000 K. At 1273 K, the amount of Al in the liquid in equilibria with both carbides was found to be greater than 13.3 wt% [60] but could not be determined accurately due to reactivity issues between the samples and the Ta crucibles. It is noteworthy that both at 1000 K and 1273 K the carbon content in the liquid was too low to be measured by WDS or EDS. Then, Viala et al. [3] measured tie-lines between Al_4C_3 and the liquid phase. Paradoxically, the Mg content in solid solution in Al_4C_3 was sometimes reported to decrease with increasing Mg content in the liquid. For instance, Mg amount in Al_4C_3 was measured at 5.6, 6.1 and 5.1 wt% when being in equilibrium with a liquid containing respectively 23, 22 and 21 wt%Al. This inconsistency can be explained by the fact Al_4C_3 crystals are platelet shape and that the matrix is therefore likely to influence the WDS measurements leading to an overestimation of the Mg content. Hence, those raw results were not selected in the present assessment. Instead, the amount of Mg in Al_4C_3 at 1000 K in three-phase equilibria with liquid and T2-Al_2MgC_2 was estimated from the three closest measurements mentioned above at 5.6±1.8 wt% in an extended uncertainty with a 0.95 confidence level.

3. Determination of the thermal stability of T2-Al_2MgC_2

3.1 Materials and methods

Differential thermal analysis (DTA) was performed on samples synthesized from the composition 70Mg – 19Al – 11C wt% in sealed Ta crucibles at 1273 K for 240 hours before being quenched in water. After synthesis, stoichiometric T2-Al_2MgC_2 crystals were obtained in a 97.7Mg – 2.3Al wt% matrix along with graphite and MgO as the main impurity. Extensive details on the materials, methods and characterizations of samples are available elsewhere [2].

The DTA were performed in a SETARAM TAG92 apparatus using a differential scanning calorimetry (DSC) cell equipped with type B thermocouple (Pt-30Rh/Pt-6Rh). The samples were contained in sealed Ta crucibles with a thickness of 0.5 mm designed to withstand the Mg vapor pressure at high temperature. A tungsten cylinder prepared so that its thermal mass would be roughly similar to the one of the samples at 1200 K was used as a reference. A thinner W cylinder was preferred to a Ta crucible as a reference in order to better fit the present DSC cell geometry. Both the crucibles, the reference and the DSC sensor were painted by an yttrium oxide paste to avoid any mutual reaction. The measurements were carried out under a dynamic flow of Ar after several purges. Oxidation of the crucibles and of the reference was avoided as the weight variation measured during the analysis were negligible. The samples were heated from room temperature to 1673 K at a speed of 10 $K.min^{-1}$. Beyond this temperature, analysis were not attempted as the crucibles might have failed under the Mg vapor pressure. Calibrations in temperature were performed using Cu, Ag and Au samples contained in Ta crucibles. An attempt to use Si failed due to reactivity issues with the crucibles. The melting temperature for the standards was taken from the international temperature scale of 1990 [61]. A linear regression was determined between 1235.07 and 1358.31 K for the three standard with a coefficient of determination of 0.9999 and the uncertainty inherent in the temperature measurements was estimated to be ±0.5 K.

3.2 Results and discussion

Thermograms obtained for two different samples are presented in Fig. 1. Thermal arrests were recorded when the signal would come off from the baseline.

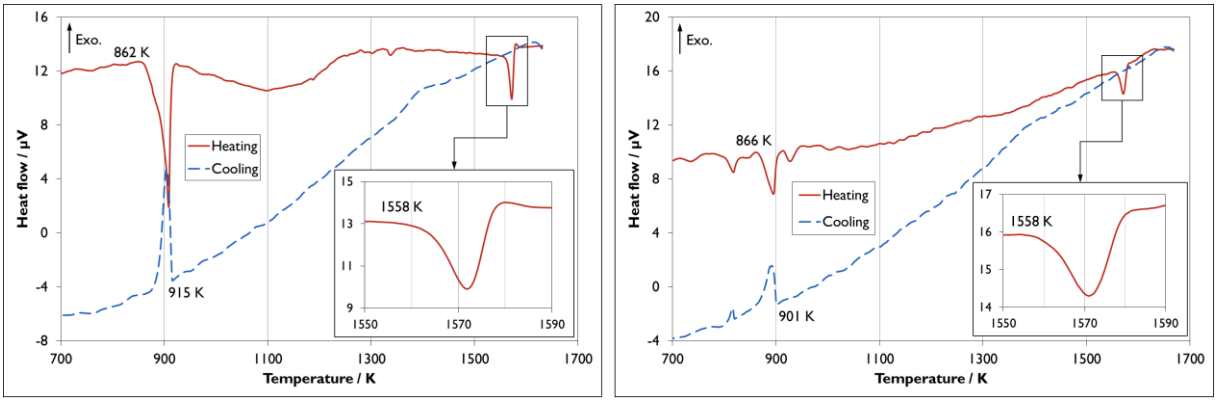

Fig. 1 Thermograms obtained from the DTA performed on two different 70Mg-19Al-11C wt% samples equilibrated at 1273 K for 240 hours

First of all, the thermal arrests obtained on both thermograms presented in Fig. 1 at roughly 865 K when heating and 910 K when cooling are attributed to melting of the Mg-Al matrix. According to the COST 507 Al-Mg description [55], the temperature of 865 K recorded when heating match with a solidus of 3.2 wt%Al, and the one of 910 K when cooling with a liquidus of 2.6 wt%Al. This is in good agreement with the composition of 2.3 wt%Al measured before DTA [2]. After melting of the Mg matrix, according to the initial sample composition and to the reported isothermal section of Viala et al. [3], a three-phase equilibria with graphite and Al_2MgC_2 is

obtained. Then, the Al content of the liquid involved in this ternary equilibrium was reported [2,3] to increase with the temperature. Therefore, Al_2MgC_2 start to decompose along a monovariant line to form graphite and an Al richer liquid. However, this phenomenon can hardly be distinguished from the irregular baseline. Finally, the endothermic thermal arrest observed at roughly 1560 K was attributed to the peritectic decomposition of Al_2MgC_2 to form graphite, Al_4C_3 and a liquid. It has to be noted that reversibility of the Al_2MgC_2 decomposition was not visible on the cooling curves.

The microstructure observed by SEM before and after DTA presented on Fig. 2 support the fact that decomposition of Al_2MgC_2 occurred, led to formation of Al_4C_3, and was not reversible during cooling. Indeed, the T2-Al_2MgC_2 crystals observed before DTA were replaced by Al_4C_3 crystals of rather different morphology. The lack of reversibility is not surprising and commonly observed in the case of peritectic reactions. It is noteworthy that after DTA a few Al_2MgC_2 crystals could be found trapped in the middle of the biggest Al_4C_3 crystals [40]. Moreover, it is suggested that the films observed around the T2-Al_2MgC_2 phase in Fig. 2a are artefacts from the polishing procedure.

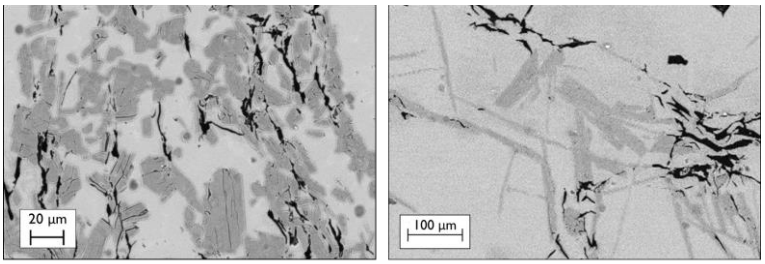

Fig. 2 BSE imaging of the 70Mg-19Al-11C wt% sample before and after DTA. (a) Before DTA, the microstructure is characterized by rectangular T2-Al_2MgC_2 crystals (dark grey), graphite (black) and a few round MgO particles (dark grey) in a Mg rich matrix (light grey). (b) After DTA, the microstructure is characterized by needle shaped Al_4C_3 containing roughly 4wt%Mg, graphite (black) and a few round MgO particles (dark grey) in a Mg rich matrix (light grey).

Besides, it is noted that the baseline of the thermograms presented in Fig. 1 is irregular due to the experimental set-up, and notably to the rather thick homemade Ta crucibles designed to withstand Mg vapor pressure during the analysis. Indeed, it should be emphasized again here that experimental work in the Mg-Al-C system is delicate. Therefore, the small and round thermal arrests observed when heating at roughly 1330 K and 920 K for samples (a) and (b) respectively were considered to be measurements artefacts as they were not reproducible. It is difficult to assess whether the thermal arrests obtained for thermogram (b) at roughly 800 K at both heating and cooling are artefacts or not and it would require further analysis.

In conclusion, sharp and reproducible thermal arrests were obtained at roughly 1560 K when heating samples containing T2-Al_2MgC_2, an Mg-Al matrix, and graphite. They were attributed to the invariant decomposition of T2-Al_2MgC_2 as supported by SEM-EDS characterizations. The corresponding invariant temperature was determined based on 4 measurements at 1559±10 K with an expanded uncertainty with a 0.95 confidence level on the basis of a two-sided Student's t-distribution with three degrees of freedom. It is noteworthy that the measurements were performed under roughly 3.4 bar of pressure although its influence on the equilibria of condensed phases (liquid, Al_4C_3, Al_2MgC_2, graphite) is considered largely negligible.

4. Determination of the end-members of the Mg solution in Al_4C_3

In order to model the Mg solution in Al_4C_3, it is important to precise the substitution site in the crystallographic structure. The coordinates of atoms in the Al_4C_3 structure as determined by single-crystal XRD by Gesing and Jeitschko [48] are detailed in Table 2. Results from Viala et al. [3] clearly shown that Mg substitute exclusively to Al. However, there are two different crystallographic positions available for Al in the Al_4C_3 structure, namely Al1 and Al2, and both having the same multiplicity. Therefore, three end-members were considered in this work, namely $Mg_2Al_2C_3$ when Mg substitute on the Al1 site, $Al_2Mg_2C_3$ when on the Al2 site and Mg_4C_3 when on both sites.

Table 2 Coordinates of atoms in Al_4C_3 (space group 166, R-3m) as determined by [48]

Atom	Wyckoff position	Site symmetry	x	y	z
Al1	6c	3m	0	0	0.29422(6)
Al2	6c	3m	0	0	0.12967(7)
C1	3a	-3m	0	0	0
C2	6c	3m	0	0	0.2168(2)

The standard enthalpy of formation of those end-members was investigated by DFT. The Strongly Conditioned and Appropriately Normed (SCAN) semi-local density functional [58,59] was selected in compliance with previous work performed on Al_4C_3 [1] and T2-Al_2MgC_2 [2]. Extensive details on the calculations can be found elsewhere [1,2]. It is to note that Zero Point Energy (ZPE) correction were not performed in this work as phonon calculations were not conducted. In addition, a corrections of -4.9 kJ.mol of graphite^{-1} was applied to account for the difference between the calculations and the experimental work and as discussed by Pisch et al. [1].

The results of DFT calculations presented in Table 3 clearly indicate that the substitution of Mg on the Al2 crystallographic site of Al_4C_3 is favored as the corresponding end-member $Al_2Mg_2C_3$ is even predicted to be stable with respect to the elements at 0K.

Table 3 Calculated ground state energy and enthalpy of formation at 0K for the potential end-member of the Mg solution in Al_4C_3

End-member	E / kJ.mol^{-1}	Δ_fH / kJ.mol^{-1}	Corrected Δ_fH (graphite) / kJ.mol^{-1}	Corrected Δ_fH (graphite) / kJ.mol of atoms^{-1}
$Mg_2Al_2C_3$	-4932.2	+406.1	+391.5	+55.9
$Al_2Mg_2C_3$	-5101.2	+2.5	-12.2	-1.7
Mg_4C_3	-4140.4	+655.2	+640.6	+91.5

5. Thermodynamic modeling and optimisation procedure

Only Al_2MgC_2, the liquid phase, and the Mg solubility in Al_4C_3 were modeled in this work. Polymorphic transition of Al_2MgC_2 was not considered due to a lack of data on the T1 low-temperature form, however as mentioned earlier both T1 and T2 polymorphs should be very close in an energetic point of view. Therefore, in a first approximation, the thermodynamic and phase equilibria data in the temperature range of existence of T1-Al_2MgC_2 (T<1000 K) calculated based on the available data on the T2 form are considered to be reasonable predictions. The Gibbs energies of the pure elements were taken from the SGTE database [63]. Regarding the binaries, the C-Mg system was taken from Chen et al. [56], Al-Mg from the COST507 database [55] and Al-C from the recent revision proposed by the Deffrennes et al. [39]. All calculations were performed using both software packages Pandat [64] and Thermocalc [65], and the results were checked for agreement.

The Al_2MgC_2 carbide was treated as a stoichiometric phase and its Gibbs energy was modeled according to Eq. 1. The expression for the heat capacity of the phase is given in Eq. 2 from Eq. 1.

$$G_m^{Al_2MgC_2}(T) - 2H_{Al}^{SER} - H_{Mg}^{SER} - 2H_C^{SER} = A + BT + CT\ln(T) + DT^2 + ET^{-1} + FT^3 \quad (1)$$

$$C_p^{Al_2MgC_2}(T) = -C - 2DT - 2ET^{-2} - 6FT^2 \quad (2)$$

The Liquid phase was treated as a substitutional solution (Al, C, Mg). The binary interaction parameters were extrapolated by the Kohler/Toop method [66] with C being the Toop element. No ternary excess parameters were used.

Mg solubility in Al_4C_3 was modeled using the Compound Energy Formalism (CEF) [67] with the formula $(Al)_2(Al,Mg)_2C_3$ selected in accordance with the fact that Mg preferentially substitute on the Al2 site (cf. Section 4). The end-member phase $Al_2Mg_2C_3$ was modeled using a floating reference according to Eq. 3 and the reference term of the phase Gibbs energy is presented in Eq. 4. A Redlich-Kister series [68] was used to model the excess Gibbs energy of $(Al)_2(Al,Mg)_2C_3$. The excess term is presented in Eq. 5 and the Redlich-Kister interaction parameters in Eq. 6.

$$G_m^{Al_2Mg_2C_3}(T) = 2G_m^{Al-fcc} + 2G_m^{Mg-hcp} + 3G_m^{C-graphite} + A \quad (3)$$

$$^{ref}G_m^{Al_2(Al,Mg)_2C_3}(T) = y_{Al}^{(1)}y_{Al}^{(2)}y_C^{(3)}G_m^{Al_4C_3}(T) + y_{Al}^{(1)}y_{Mg}^{(2)}y_C^{(3)}G_m^{Al_2Mg_2C_3}(T) \quad (4)$$

$$^{ex}G_m^{Al_2(Al,Mg)_2C_3}(T) = y_{Al}^{(1)}y_{Al}^{(2)}y_{Mg}^{(2)}y_C^{(3)}\ {}^0L_{Al:Al,Mg:C}^{(Al)_2(Al,Mg)_2(C)_3} \quad (5)$$

$${}^0L_{Al:Al,Mg:C}^{(Al)_2(Al,Mg)_2(C)_3} = {}^0a_{Al:Al,Mg:C} + {}^0b_{Al:Al,Mg:C}T \quad (6)$$

In a first stage, the thermodynamic properties of Al_2MgC_2 were modeled. First of all, the C, D, E and F coefficients of Eq. 2 were determined using the heat capacity of T2-Al_2MgC_2 calculated by DFT in the quasi-harmonic approximation [2]. Three temperature ranges were used to describe the heat capacity of Al_2MgC_2 in order to reduce the number of parameters and to avoid aberrations at extreme temperatures caused by the use of the powers of T terms. Then, the B coefficient of Eq. 1 was adjusted using the standard entropy of formation of T2-Al_2MgC_2 ($\Delta_fS°_{298}$) calculated by DFT [2]. For the last temperature range, the parameter B was determined using the condition of continuity of the entropy function of Al_2MgC_2. Finally, the A coefficient of Eq. 1 was adjusted using the DFT standard enthalpy of formation of T2-Al_2MgC_2 ($\Delta_fH°_{298}$) [2] and this parameter was determined for the last temperature range using the condition of continuity of the Gibbs energy function of Al_2MgC_2.

In a second and final stage, a joint optimization of the parameters regarding the end-member $Al_2Mg_2C_3$, the phase $(Al)_2(Al,Mg)_2(C)_3$, and the last temperature range of Al_2MgC_2 was performed. In addition to the T2-Al_2MgC_2 data already mentioned above, the temperature of invariant decomposition of Al_2MgC_2 measured in this work was used along with phase equilibria data determined by Viala et al. [3] and the DFT standard enthalpy of formation of $Al_2Mg_2C_3$. A high weight was selected for the calculated entropy of formation of Al_2MgC_2 during this process, and the continuity over the different temperature ranges of the thermodynamic functions of the ternary carbide was ensured afterwards. Extensive details regarding the uncertainties and the weights used in the optimization can be found elsewhere [60].

The thermodynamic parameters obtained in the present modeling are presented in Table 4.

Table 4 Thermodynamic parameters given in J.mol^{-1} in the form A + BT + CTln(T) + DT^2 + ET^{-1} + FT^3

Term	T-range	A	B	C	D.10^3	E.10^{-6}	F.10^6
Al_2MgC_2, Stoichiometric, Al_2MgC_2							
$G_m^{Al_2MgC_2} - 2H_{Al}^{SER} - H_{Mg}^{SER} - 2H_C^{SER}$	50-298.15K	-137023.17	-130.2133	+31.64858	-309.8213	-0.009339	+123.3135
	298.15-500K	-141504.37	+95.31393	-11.48743	-168.8773	-	+46.2193
	500-3000K	-170910.3	+715.88624	-113.83391	-9.9976	+1.599446	-
Al_4C_3, Compound Energy Formalism, $(Al)_2(Al,Mg)_2(C)_3$							
$G_m^{Al_2Mg_2C_3} - 2G_m^{Al-fcc} - 2G_m^{Mg-hcp} - 3G_m^{C-graphite}$	50-2000K	-13540	-				
${}^0L_{Al:Al,Mg:C}^{(Al)_2(Al,Mg)_2(C)_3}$	50-3000K	-20471	+93.252				

6. Results and discussion

6.1 Thermodynamic properties

The heat capacity of Al_2MgC_2 calculated with the parameters in Table 3 is presented in Fig. 3 along with the DFT and DSC data on the T2 form [2]. For clarity reasons, only one third of the experimental points are plotted in the figure. The fit obtained in this work is in perfect agreement with DFT calculations from 50 to 400 K and deviate slightly from it at higher temperature. This deviation was allowed to compensate for the fact that the DFT heat capacity is probably underestimated as anharmonic contributions rise with temperature. The difference of roughly 3% observed at 1000 K is consistent with the order of magnitude of the anharmonic contributions observed for the Al_4C_3 phase [1] and the fit obtained is still within the experimental uncertainties.

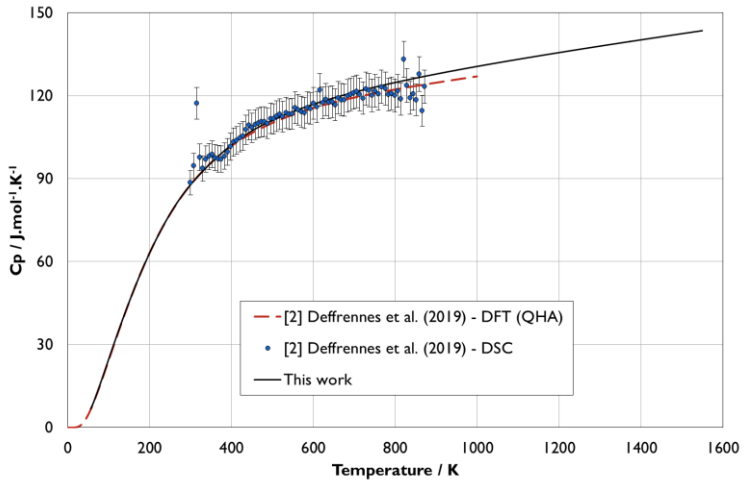

Fig. 3 Calculated heat capacity of Al_2MgC_2 compared with DSC measurements and DFT calculations on T2-Al_2MgC_2 from [2]

The calculated standard entropy and enthalpy of formation of Al_2MgC_2 are compared with the literature data on the T2 form in Table 5. The standard entropy of formation is in a perfect match with the DFT value of 70.0 $J.K^{-1}.mol^{-1}$ [2]. Regarding the standard enthalpy of formation, an optimized value of -25.1 kJ.mol of $atoms^{-1}$ was obtained, this result being 1.5 kJ.mol of $atoms^{-1}$ more exothermic than the results from DFT calculations. It is noted that a similar discrepancy of 1.4 kJ.mol of $atoms^{-1}$ was obtained between the DFT and the optimized standard enthalpy of formation of Al_4C_3 when modeling the Al-C binary system [39]. It is also interesting to highlight that using previous versions of the Al-C binary [69–71], the enthalpy of formation of Al_2MgC_2 would have been roughly 5 kJ.mol of $atoms^{-1}$ more exothermic than the DFT value so that the phase equilibria data could be fit satisfactorily.

Table 5 Calculated standard enthalpy and entropy of formation of T2-Al_2MgC_2 compared with DFT calculations from [2]

Reference	$\Delta_f H°_{298.15\ k}$ / kJ.mol of $atoms^{-1}$	$\Delta_f S°_{298.15\ K}$ / $J.K^{-1}.mol^{-1}$
19Def	-23.6	70.0
This work	-25.1	70.0

Regarding the enthalpy of formation of the end-member phase $Al_2Mg_2C_3$, an optimized value of -1.9 kJ.mol of $atoms^{-1}$ was obtained, which is only -0.2 kJ.mol of $atoms^{-1}$ more exothermic than the DFT calculations at 0K. It is noteworthy that this value has very limited influence in the overall results as it can be easily compensated by the interaction parameters.

6.2 Phase equilibria

It is reminded here that polymorphic transition of Al_2MgC_2 could not be taken into account and that the phase was modeled based on the data regarding its T2 form, yet that the calculated equilibria involving the low-temperature T1 form, partially stable below 1000K, are considered to be reasonable predictions. Therefore, the ternary carbide is simply denoted as Al_2MgC_2 in the following sections. In addition, the aluminum carbide can contain variable amount of Mg in solid solution but will simply be referred to as Al_4C_3.

Isothermal sections of the ternary phase diagram at 1000 and 1273 K are presented in Fig. 4. At 1000 K, the agreement between the calculated and the experimental phase equilibria determined by Viala et al. [3] is very satisfying. The Al content in the liquid in three-phase equilibrium liquid + graphite + Al_2MgC_2 was calculated at 0.5 wt% Al which is in good agreement with the experimental value of 0.6±2wt%. The liquid composition in the liquid + Al_2MgC_2 + Al_4C_3 equilibrium is calculated at 18.5 wt% Al, which compares well to the 19±2wt% determined by Viala et al. [3]. Finally, the content of Mg in solid solution in Al_4C_3 when the phase is in equilibrium with liquid and Al_2MgC_2 was calculated at 5.2 wt% Mg which is in good agreement with the value of 5.6±1.8 wt% estimated in the present study from the measurements of Viala et al. [3]. At 1273 K, the liquid composition in the liquid + graphite + Al_2MgC_2 equilibrium was calculated at 2.8 wt% Al, which is in good agreement with the value of 2.3 wt% measured by EDS [2].

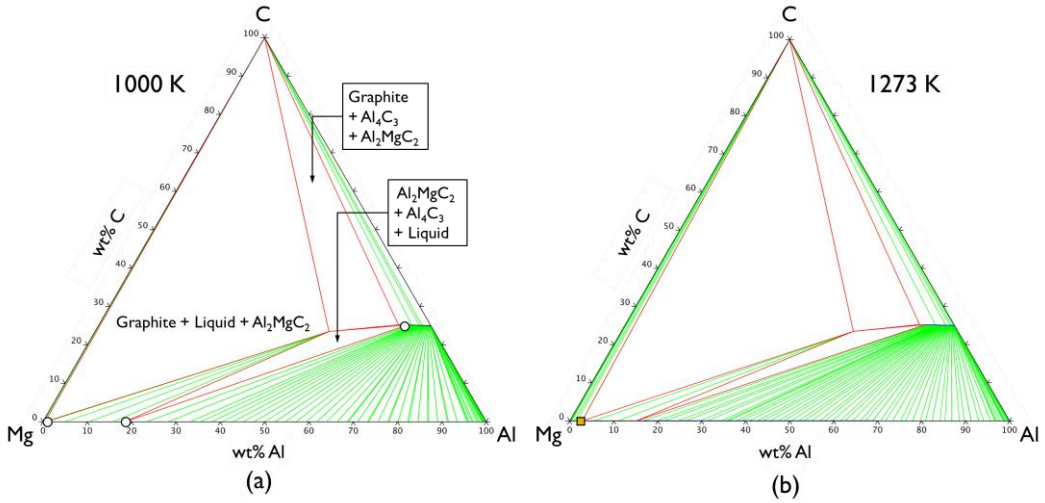

Fig. 4 Isothermal sections of the Al-C-Mg system calculated at (a) 1000 K and (b) 1273 K. Open circles represent the data measured by Viala et al. [3] at 1000 K and filled square by Deffrennes et al. [2] at 1273 K

The calculated liquidus projection is presented in Fig. 5, and more details regarding the highlighted ternary invariant equilibria are given in Tables 6 and 7. The solubility of Mg in Al_4C_3 is predicted to increase up to 8.8 wt% Mg at 1550 K and then to decrease down to 0 when Al_4C_3 decomposes at 2410.7 K as calculated in the Al-C binary [39]. The invariant decomposition temperature of Al_2MgC_2 determined by DTA at 1559±10 K is in satisfying agreement with the modeled value of 1550 K and the liquid involved was calculated to contain 11.3 wt% Al and 0.2 wt% C. The monovariant line liquid + Graphite + (Mg) pointing from the Mg-C binary eutectic down towards the invariant U_1 almost collapses to a point at the y-axis in Fig. 5. Even though U_1 is almost degenerate, it is clearly a transition type reaction because the liquid composition at U_1 is located outside the triangle of the solid phases Graphite = (Mg) + Al_2MgC_2. There is no maximum in the monovariant line from U_1 to U_2.

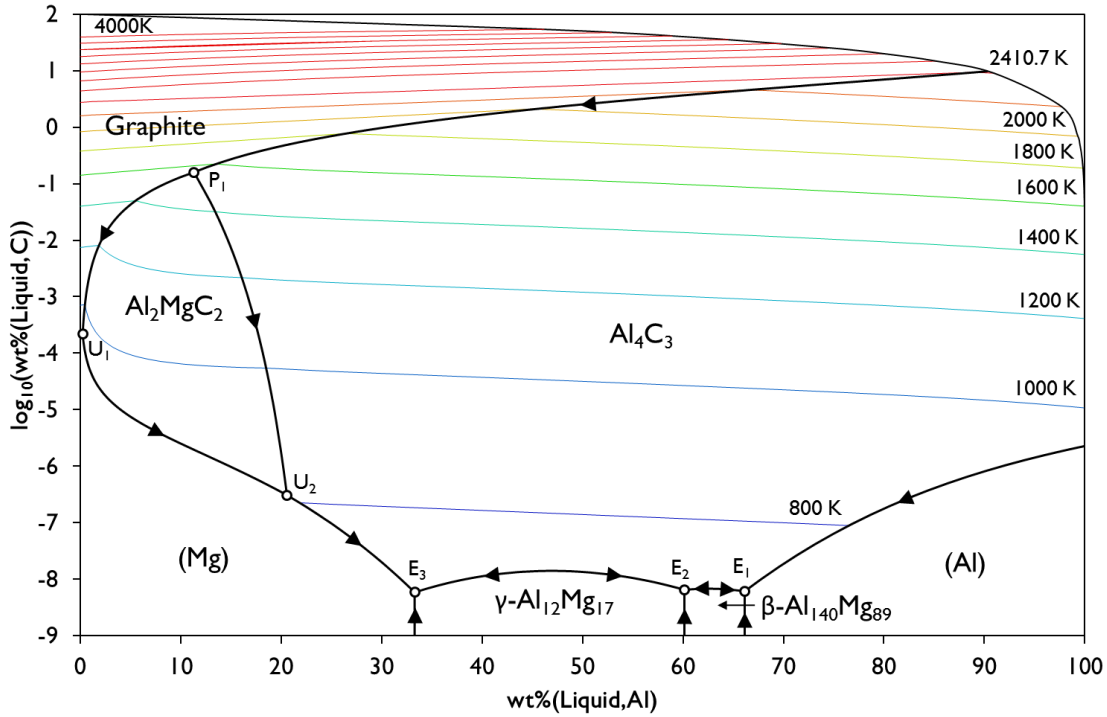

Fig. 5 The calculated Al-C-Mg liquidus projection, disregarding the gas phase. On the y-axis a logarithmic representation of the carbon content in the liquid phase is plotted to enlarge the region of interest around the invariant reactions. The binary Al-C edge converts to a curved shape, where the peritectic Liquid + Graphite = Al_4C_3 is seen at 2410.7 K.

Table 6 Calculated invariant reactions in the ternary system Al-C-Mg. ΔT denotes the difference between the corresponding binary and the (almost) degenerate ternary invariant reactions.

Reaction	Reaction type	T / K	ΔT / K
P_1 : Liquid + Al_4C_3 + Graphite = Al_2MgC_2	Peritectic	1549.6	N.A.
U_1 : Liquid + Graphite = (Mg) + Al_2MgC_2	Transition	921.8	1.2
U_2 : Liquid + Al_2MgC_2 = Al_4C_3 + (Mg)	Transition	808.5	N.A.
E_1 : Liquid = β-$Al_{140}Mg_{89}$ + (Al) + Al_4C_3	Eutectic	723.6	1E-7
E_2 : Liquid = β-$Al_{140}Mg_{89}$ + γ-$Al_{12}Mg_{17}$ + Al_4C_3	Eutectic	722.7	1E-7
E_3 : Liquid = γ-$Al_{12}Mg_{17}$ + (Mg) + Al_4C_3	Eutectic	709.4	1E-7

Table 7 Calculated composition in wt.% (at.%) of the phases involved in the non-degenerate ternary invariants

	Al_2MgC_2		Al_4C_3		Graphite		Liquid		(Mg)	
Invariant	Al	C	Al	C	Al	C	Al	C	Al	C
P_1	52.8 (40.0)	23.5 (40.0)	65.9 (49.8)	25.3 (42.9)	0.0 (0.0)	100.0 (100.0)	11.3 (10.3)	0.2 (0.3)	-	-
U_2	52.8 (40.0)	23.5 (40.0)	70.3 (53.3)	25.2 (42.9)	-	-	20.6 (18.9)	3.1E-7 (6.4E-7)	6.1 (5.6)	0.0 (0.0)

7 Application to the grain refinement of Mg-Al alloys by carbon inoculation

In this section, the phase formation sequence during solidification of a classical Mg-9Al wt% alloy inoculated with 0.5 wt% C at 1000 K is predicted based on the present modeling of the ternary system. For this composition, Al_2MgC_2 is obtained to be the only stable compound from 809 to 1376 K where the gas phase starts forming at 1 bar. Under higher pressure, Al_2MgC_2 may be stable up to about 1500 K where transformation

to graphite is predicted on further heating, as also seen in Fig. 5. In order to be in equilibrium with Al_4C_3 at 1000 K the liquid should contain more than 18.5 wt% Al which is far beyond the composition of industrial Mg alloys.

Assuming an initial equilibration of Mg-9Al wt% alloy with 0.5 wt% C addition at 1000 K the two phases liquid + Al_2MgC_2 form during a holding time of typically 20 minutes at the inoculation temperature. The mass fraction of 0.021 of this initial Al_2MgC_2-formation results in drastically reduced content of dissolved carbon, 0.00007 wt% C, in the equilibrated liquid with fraction 0.979 and composition Mg-8.048Al-0.00007C (wt%). The fraction of this initial Al_2MgC_2 changes only little with temperature, from 0.0208 at 1300 K to 0.0213 at 900 K. The phase formation during casting of this liquid may then be predicted by Scheil-Gulliver solidification simulation of the liquid starting at 1000 K and disregarding the initially formed Al_2MgC_2. The phase fraction evolution is presented in Fig. 6. The solidification of (Mg) is predicted to start at 881 K with Al_2MgC_2 being the dominant carbide present in the liquid phase. The phase fraction of the secondary Al_2MgC_2 grows from zero at 1000 K to about $3 \cdot 10^{-6}$ as seen in Fig. 6b. Only a negligible amount of Al_4C_3, less than $3 \cdot 10^{-9}$, is formed in Scheil conditions below 809 K, after most of the liquid, fraction 0.74, already solidified. Scheil solidification is predicted to end at 709 K in the ternary eutectic E_3 by the formation of γ-$Al_{12}Mg_{17}$ (fraction of 0.09) together with (Mg), see Fig. 6a.

It is important to note that both the initial Al_2MgC_2, predicted with mass fraction of 0.021, and the small fraction of secondary Al_2MgC_2, presumably growing on it, should be considered as active nucleant. Therefore, it is essential to provide a sufficient amount of carbon addition to the melt during holding at about 1000 K. The simulated growth of secondary Al_2MgC_2 shown in Fig. 6 will be essentially the same even if much less than 0.5 wt% C is added, assuming it is more than the very small carbon solubility limit in the liquid.

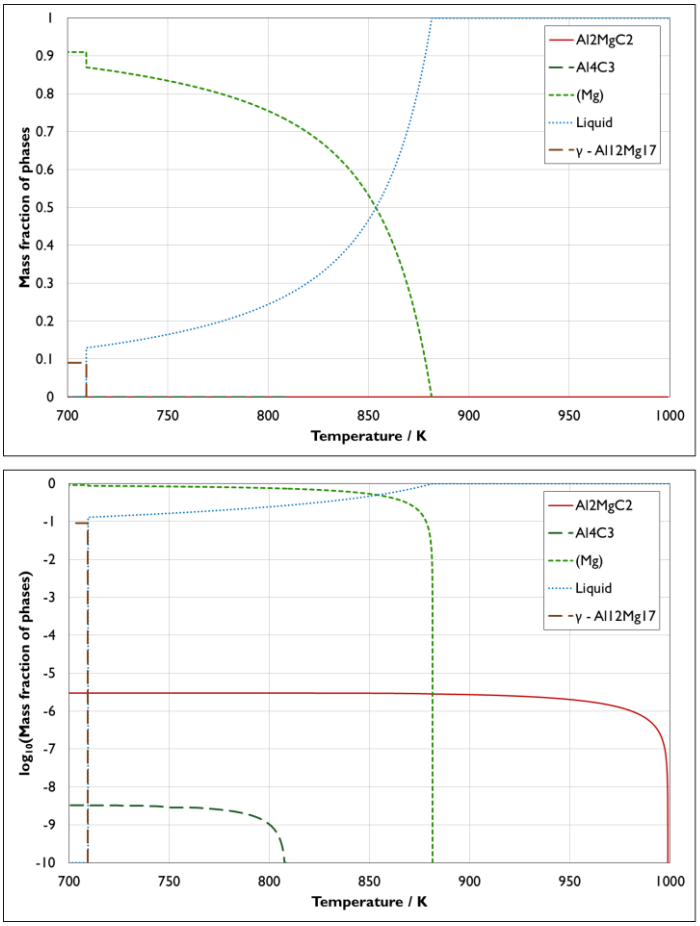

Fig. 6 Mass fraction of phases obtained from Scheil solidification simulation of a 91Mg-9Al wt% alloy inoculated by 0.5 wt%C at 1000K plotted with (a) a linear representation and (b) a logarithmic representation

In conclusion, thermodynamic calculations provide a convincing argument that Al_2MgC_2 is the nucleant responsible for the grain refinement of Mg-Al alloys inoculated by carbon. A very interesting perspective lies in the inclusion of the present modeling to the Mg thermodynamic databases in order to investigate the effect of alloying elements on the phase formation, notably for the case of Mn highlighted in the introduction.

8. Conclusions

In the present work the temperature of the peritectic decomposition of Al_2MgC_2 was determined at 1559±10 K by DTA. DFT calculations were conducted on potential end-member phases of the Mg solution in Al_4C_3 and it was shown that the substitution of Mg on the Al2 site of the structure was the only energetically favorable substitution. Based on those findings as well as on previous work of the authors, a CALPHAD modeling of the ternary Al-C-Mg system was conducted. Due to the phase equilibria data taken into account, the optimization was rather constraint and the very satisfying agreement obtained with experimental data demonstrates the self-consistency of the proposed description. The present assessment provides the basis to support the development of Mg-Al alloys and composites.

Acknowledgments

This research did not receive any specific grant from funding agencies in the public, commercial, or not-for-profit sectors. The authors wish to thank the GDR CNRS n°3584 (TherMatHT) community where fruitful discussions led to collaboration on this project. The assistance of members of the "Centre Technologique des Microstructures, Université Lyon 1" (CTμ, http://microscopies.univ-lyon1.fr) for SEM characterizations is gratefully acknowledged.

Data availability

The datasets analyzed during the current study will be made available from the corresponding author on request.

References

[1] A. Pisch, A. Pasturel, G. Deffrennes, O. Dezellus, G. Mikaelian, P. Benigni, Investigation of the thermodynamic properties of Al4C3: a combined DFT and DSC study, Manuscript Submitted for Publication. (2019).

[2] G. Deffrennes, B. Gardiola, E. Jeanneau, A. Pisch, A. Pasturel, G. Mikaelian, P. Benigni, J. Andrieux, O. Dezellus, Synthesis, crystallographic structure and thermodynamic properties of T2-Al2MgC2, Journal of Solid State Chemistry. (2019). doi:10.1016/j.jssc.2019.02.039.

[3] J.C. Viala, G. Claveyrolas, F. Bosselet, J. Bouix, The chemical behaviour of carbon fibres in magnesium base Mg-Al alloys, Journal of Materials Science. 35 (2000) 1813–1825.

[4] V.M. Hong Ng, H. Huang, K. Zhou, P.S. Lee, W. Que, J.Z. Xu, L.B. Kong, Recent progress in layered transition metal carbides and/or nitrides (MXenes) and their composites: synthesis and applications, Journal of Materials Chemistry A. 5 (2017) 3039–3068. doi:10.1039/C6TA06772G.

[5] O. Mashtalir, M. Naguib, V.N. Mochalin, Y. Dall'Agnese, M. Heon, M.W. Barsoum, Y. Gogotsi, Intercalation and delamination of layered carbides and carbonitrides, Nature Communications. 4 (2013). doi:10.1038/ncomms2664.

[6] A. Dey, K.M. Pandey, Magnesium Metal Matrix Composites - A Review, Reviews on Advanced Materials Science. 42 (2015) 58–67.

[7] A. Hähnel, E. Pippel, A. Feldhoff, R. Schneider, J. Woltersdorf, Reaction layers in MMCs and CMCs: structure, composition and mechanical properties, Materials Science and Engineering: A. 237 (1997) 173–179. doi:10.1016/S0921-5093(97)00127-5.

[8] H. Fukuda, K. Kondoh, J. Umeda, B. Fugetsu, Interfacial analysis between Mg matrix and carbon nanotubes in Mg–6wt.% Al alloy matrix composites reinforced with carbon nanotubes, Composites Science and Technology. 71 (2011) 705–709. doi:10.1016/j.compscitech.2011.01.015.

[9] A. Feldhoff, E. Pippel, J. Woltersdorf, Carbon-fibre reinforced magnesium alloys: nanostructure and chemistry of interlayers and their effect on mechanical properties, Journal of Microscopy. 196 (1999) 185–193. doi:10.1046/j.1365-2818.1999.00618.x.

[10] A. Feldhoff, E. Pippel, J. Wolterdorf, Interface Engineering of Carbon-Fiber Reinforced Mg-Al Alloys, Advanced Engineering Materials. 2 (2000) 471–480. doi:10.1002/1527-2648(200008)2:8<471::AID-ADEM471>3.0.CO;2-S.
[11] K. Kondoh, H. Fukuda, J. Umeda, H. Imai, B. Fugetsu, Microstructural and mechanical behavior of multi-walled carbon nanotubes reinforced Al–Mg–Si alloy composites in aging treatment, Carbon. 72 (2014) 15–21. doi:10.1016/j.carbon.2014.01.013.
[12] C.H. Caceres, G.E. Mann, J.R. Griffiths, Grain Size Hardening in Mg and Mg-Zn Solid Solutions, Metallurgical and Materials Transactions A. 42 (2011) 1950–1959. doi:10.1007/s11661-010-0599-2.
[13] M. Suresh, A. Srinivasan, K.R. Ravi, U.T.S. Pillai, B.C. Pai, Microstructural refinement and tensile properties enhancement of Mg–3Al alloy using charcoal additions, Materials Science and Engineering: A. 528 (2011) 2502–2508. doi:10.1016/j.msea.2010.12.008.
[14] M. Suresh, A. Srinivasan, U.T.S. Pillai, B.C. Pai, Mechanism for Grain Refinement and Mechanical Properties of AZ91 Mg Alloy by Carbon Inoculation, Procedia Engineering. 55 (2013) 93–97. doi:10.1016/j.proeng.2013.03.225.
[15] J. Du, J. Yang, M. Kuwabara, W. Li, J. Peng, Effects of Carbon and/or Alkaline Earth Elements on Grain Refinement and Tensile Strength of AZ31 Alloy, MATERIALS TRANSACTIONS. 49 (2008) 2303–2309. doi:10.2320/matertrans.MRA2008146.
[16] C.J. Bettles, M.A. Gibson, S.M. Zhu, Microstructure and mechanical behaviour of an elevated temperature Mg-rare earth based alloy, Materials Science and Engineering: A. 505 (2009) 6–12. doi:10.1016/j.msea.2008.11.004.
[17] K.D. Ralston, N. Birbilis, Effect of Grain Size on Corrosion: A Review, CORROSION. 66 (2010) 075005-075005–13. doi:10.5006/1.3462912.
[18] M.R. Barnett, A.G. Beer, D. Atwell, A. Oudin, Influence of grain size on hot working stresses and microstructures in Mg–3Al–1Zn, Scripta Materialia. 51 (2004) 19–24. doi:10.1016/j.scriptamat.2004.03.023.
[19] L. Wang, Y.M. Kim, J. Lee, B.S. You, Improvement in rollability of AZ91 magnesium alloy by carbon addition, Materials Science and Engineering: A. 528 (2011) 943–949. doi:10.1016/j.msea.2010.10.069.
[20] Q. Jin, J.-P. Eom, S.-G. Lim, W.-W. Park, B.-S. You, Grain refining mechanism of a carbon addition method in a Mg–Al magnesium alloy, Scripta Materialia. 49 (2003) 1129–1132. doi:10.1016/j.scriptamat.2003.07.001.
[21] M. Qian, P. Cao, Discussions on grain refinement of magnesium alloys by carbon inoculation, Scripta Materialia. 52 (2005) 415–419. doi:10.1016/j.scriptamat.2004.10.014.
[22] Q. Jin, J.-P. Eom, S.-G. Lim, W.-W. Park, B.-S. You, Reply to comments on "Grain refining mechanism of a carbon addition method in a Mg–Al magnesium alloy," Scripta Materialia. 52 (2005) 421–423. doi:10.1016/j.scriptamat.2004.10.030.
[23] Y.M. Kim, C.D. Yim, B.S. You, Grain refining mechanism in Mg–Al base alloys with carbon addition, Scripta Materialia. 57 (2007) 691–694. doi:10.1016/j.scriptamat.2007.06.044.
[24] L. Lu, A.K. Dahle, D.H. StJohn, Heterogeneous nucleation of Mg–Al alloys, Scripta Materialia. 54 (2006) 2197–2201. doi:10.1016/j.scriptamat.2006.02.048.
[25] L. Lu, A.K. Dahle, D.H. StJohn, Grain refinement efficiency and mechanism of aluminium carbide in Mg–Al alloys, Scripta Materialia. 53 (2005) 517–522. doi:10.1016/j.scriptamat.2005.05.008.
[26] S. Nimityongskul, M. Jones, H. Choi, R. Lakes, S. Kou, X. Li, Grain refining mechanisms in Mg–Al alloys with Al4C3 microparticles, Materials Science and Engineering: A. 527 (2010) 2104–2111. doi:10.1016/j.msea.2009.12.030.
[27] M.A. Easton, A. Schiffl, J.-Y. Yao, H. Kaufmann, Grain refinement of Mg–Al(–Mn) alloys by SiC additions, Scripta Materialia. 55 (2006) 379–382. doi:10.1016/j.scriptamat.2006.04.014.
[28] L. Wang, Y.M. Kim, J. Lee, B.S. You, Effect of hafnium carbide on the grain refinement of Mg-3wt.% Al alloy, Journal of Alloys and Compounds. 500 (2010) L12–L15. doi:10.1016/j.jallcom.2010.03.214.
[29] T.J. Chen, Y. Ma, W.B. Lv, Y.D. Li, Y. Hao, Grain refinement of AM60B magnesium alloy by SiC particles, Journal of Materials Science. 45 (2010) 6732–6738. doi:10.1007/s10853-010-4767-y.
[30] T. Chen, R. Wang, H. Huang, Y. Ma, Y. Hao, Grain refining technique of AM60B magnesium alloy by MgCO3, Transactions of Nonferrous Metals Society of China. 22 (2012) 1533–1539. doi:10.1016/S1003-6326(11)61352-6.
[31] K. Li, Z.G. Sun, F. Wang, N.G. Zhou, X.W. Hu, First-principles calculations on Mg/Al4C3 interfaces, Applied Surface Science. 270 (2013) 584–589. doi:10.1016/j.apsusc.2013.01.089.
[32] Y. Huang, K.U. Kainer, N. Hort, Mechanism of grain refinement of Mg–Al alloys by SiC inoculation, Scripta Materialia. 64 (2011) 793–796. doi:10.1016/j.scriptamat.2011.01.005.
[33] C. Cayron, P.A. Buffat, C. Hausmann, O. Beffort, About the epitaxial growth of Mg-subgrains on Al2MgC2 interfacial carbides in a squeeze cast Mg-4Al/T300 metal matrix composite, Journal of Materials Science Letters. 18 (1999) 1671–1674. doi:10.1023/A:1006669514604.

[34] CompuTherm PanMg, CompuTherm LLC Pandat Software PanMg2017 DATABASE (accessed 15 march 2018), 2017.
[35] Thermo-Calc TCMG, Thermo-Calc Software TCMG database version 4 (accessed 15 march 2018), 2018.
[36] FactSage FTLite, FactSage Software FTlite database version 7.2 (accessed 03 march 2018), 2018.
[37] T.I. Kosolapova, Carbides: Properties, Production, and Applications, Springer US, Boston, MA, 1995. http://dx.doi.org/10.1007/978-1-4684-8006-1 (accessed August 14, 2018).
[38] J.K. Park, J.P. Lucas, Moisture effect on SiCp/6061 Al MMC: Dissolution of interfacial Al4C3, Scripta Materialia. 37 (1997) 511–516. doi:10.1016/S1359-6462(97)00133-4.
[39] G. Deffrennes, B. Gardiola, D. Chaussende, A. Pisch, J. Andrieux, R. Schmid-Fetzer, O. Dezellus, Critical assessment and thermodynamic modeling of the Al-C system, Manuscript Submitted for Publication. (2019).
[40] G. Deffrennes, B. Gardiola, M. Lomello, J. Andrieux, O. Dezellus, R. Schmid-Fetzer, Thermodynamics of Phase Formation in Mg–Al–C Alloys Applied to Grain Refinement, in: D. Orlov, V. Joshi, K.N. Solanki, N.R. Neelameggham (Eds.), Magnesium Technology 2018, Springer International Publishing, Cham, 2018: pp. 323–327. doi:10.1007/978-3-319-72332-7_49.
[41] M.E. Straumanis, The Precision Determination of Lattice Constants by the Powder and Rotating Crystal Methods and Applications, Journal of Applied Physics. 20 (1949) 726–734. doi:10.1063/1.1698520.
[42] J.L. Murray, The Al−Mg (Aluminum−Magnesium) system, Journal of Phase Equilibria. 3 (1982). doi:10.1007/BF02873413.
[43] P. Trucano, R. Chen, Structure of graphite by neutron diffraction, Nature. 258 (1975) 136–137. doi:10.1038/258136a0.
[44] H.L. Su, M. Harmelin, P. Donnadieu, C. Baetzner, H.J. Seifert, H.L. Lukas, G. Effenberg, F. Aldinger, Experimental investigation of the Mg-Al phase diagram from 47 to 63 at.% Al, Journal of Alloys and Compounds. 247 (1997) 57–65. doi:10.1016/S0925-8388(96)02595-9.
[45] T. Czeppe, W. Zakulski, E. Bielańska, Study of the thermal stability of phases in the Mg-Al system, Journal of Phase Equilibria. 24 (2003) 249–254. doi:10.1361/105497103770330550.
[46] S. Samson, The crsytal structure of the phase β Mg_2Al_3, Acta Crystallographica. 19 (1965) 401–413. doi:10.1107/S0365110X65005133.
[47] S. Samson, E.K. Gordon, The crystal structure of ε-Mg23Al30, Acta Crystallographica Section B Structural Crystallography and Crystal Chemistry. 24 (1968) 1004–1013. doi:10.1107/S0567740868003638.
[48] T.M. Gesing, W. Jeitschko, The Crystal Structure and Chemical Properties of U2Al3C4 and Structure Refinement of Al4C3, Zeitschrift Für Naturforschung B. 50 (1995) 196–200. doi:10.1515/znb-1995-0206.
[49] F. Bosselet, B.F. Mentzen, J.C. Viala, M.A. Etoh, J. Bouix, Synthesis, and structure of T2-Al2MgC2, European Journal of Solid State and Inorganic Chemistry. 35 (1998) 91–99. doi:10.1016/S0992-4361(98)80017-9.
[50] M.-X. Zhang, P.M. Kelly, Crystallography of Mg17Al12 precipitates in AZ91D alloy, Scripta Materialia. 48 (2003) 647–652. doi:10.1016/S1359-6462(02)00555-9.
[51] M.W. Chase, National Institute of Standards and Technology (U.S.), eds., NIST-JANAF thermochemical tables, 4th ed, American Chemical Society ; American Institute of Physics for the National Institute of Standards and Technology, Washington, DC : New York, 1998.
[52] J. Abrahamson, Graphite sublimation temperatures, carbon arcs and crystallite erosion, Carbon. 12 (1974) 111–141. doi:10.1016/0008-6223(74)90019-0.
[53] A. Feldhoff, E. Pippel, J. Woltersdorf, Structure and composition of ternary carbides in carbonfibre reinforced Mg-Al alloys, Philosophical Magazine A. 79 (1999) 1263–1277. doi:10.1080/01418619908210360.
[54] M. Aljarrah, Thermodynamic Modeling and Experimental Investigation of the Mg-Al-Ca-Sr System, Concordia University, 2008.
[55] I. Ansara, A.T. Dinsdale, M.H. Rand, eds., Definition of thermochemical and thermophysical properties to provide a database for the development of new light alloys: COST 507. Vol. 2: Thermochemical database for light metal alloys, Off. for Off. Publ. of the Europ. Communities, Luxembourg, 1998.
[56] H.-L. Chen, R. Schmid-Fetzer, The Mg–C phase equilibria and their thermodynamic basis, International Journal of Materials Research. 103 (2012) 1294–1301. doi:10.3139/146.110787.
[57] H.-L. Chen, N. Li, A. Klostermeier, R. Schmid-Fetzer, Measurement of carbon solubility in magnesium alloys using GD-OES, Journal of Analytical Atomic Spectrometry. 26 (2011) 2189. doi:10.1039/c1ja10128e.
[58] J. Sun, A. Ruzsinszky, J.P. Perdew, Strongly Constrained and Appropriately Normed Semilocal Density Functional, Physical Review Letters. 115 (2015). doi:10.1103/PhysRevLett.115.036402.
[59] J. Sun, R.C. Remsing, Y. Zhang, Z. Sun, A. Ruzsinszky, H. Peng, Z. Yang, A. Paul, U. Waghmare, X. Wu, M.L. Klein, J.P. Perdew, SCAN: An Efficient Density Functional Yielding Accurate Structures and

Energies of Diversely-Bonded Materials, ArXiv:1511.01089 [Cond-Mat]. (2015). http://arxiv.org/abs/1511.01089 (accessed August 25, 2018).
[60] G. Deffrennes, Étude expérimentale et évaluation thermodynamique du système Al-C-Mg (Doctoral dissertation), Université Claude Bernard Lyon 1, Lyon, France, 2018.
[61] H. Preston-Thomas, The International Temperature Scale of 1990, Metrologia. 27 (1990) 3–10.
[62] Materials Science International Team MSIT®, Al-Cu-Mg (Aluminium - Copper - Magnesium), in: G. Effenberg, S. Ilyenko (Eds.), Light Metal Systems. Part 2, Springer-Verlag, Berlin/Heidelberg, 2005: pp. 1–32. doi:10.1007/10915967_4.
[63] A.T. Dinsdale, SGTE data for pure elements, Calphad. 15 (1991) 317–425. doi:10.1016/0364-5916(91)90030-N.
[64] W. Cao, S.-L. Chen, F. Zhang, K. Wu, Y. Yang, Y.A. Chang, R. Schmid-Fetzer, W.A. Oates, PANDAT software with PanEngine, PanOptimizer and PanPrecipitation for multi-component phase diagram calculation and materials property simulation, Calphad. 33 (2009) 328–342. doi:10.1016/j.calphad.2008.08.004.
[65] J.-O. Andersson, T. Helander, L. Höglund, P. Shi, B. Sundman, Thermo-Calc & DICTRA, computational tools for materials science, Calphad. 26 (2002) 273–312. doi:10.1016/S0364-5916(02)00037-8.
[66] P. Chartrand, A.D. Pelton, On the choice of "Geometric" thermodynamic models, Journal of Phase Equilibria. 21 (2000) 141–147. doi:10.1361/105497100770340192.
[67] M. Hillert, The compound energy formalism, Journal of Alloys and Compounds. 320 (2001) 161–176. doi:10.1016/S0925-8388(00)01481-X.
[68] O. Redlich, A.T. Kister, Algebraic Representation of Thermodynamic Properties and the Classification of Solutions, Industrial & Engineering Chemistry. 40 (1948) 345–348. doi:10.1021/ie50458a036.
[69] C. Qiu, R. Metselaar, Solubility of carbon in liquid Al and stability of Al4C3, Journal of Alloys and Compounds. 216 (1994) 55–60. doi:10.1016/0925-8388(94)91042-1.
[70] J. Gröbner, H.L. Lukas, F. Aldinger, Thermodynamic calculation of the ternary system Al-Si-C, Calphad. 20 (1996) 247–254. doi:10.1016/S0364-5916(96)00027-2.
[71] H. Ohtani, M. Yamano, M. Hasebe, Thermodynamic Analysis of the Fe-Al-C Ternary System by Incorporating ab initio Energetic Calculations into the CALPHAD Approach, ISIJ International. 44 (2004) 1738–1747. doi:10.2355/isijinternational.44.1738.